

Soft Gold Nanowire Sponges for Strain-insensitive Conductors, Wearable Energy Storage and Catalytic Converters

*Fenge Lin^{a,b}, Kaixuan Wang^{a,b}, Tiance An^{a,b}, Bowen Zhu^{a,b}, Yunzhi Ling^{a,b}, Shu Gong^{a,b},
Siyuan Liu^{a,b} and Wenlong Cheng^{a,b,*}*

^a Department of Chemical Engineering, Monash University, Clayton, 3800 Victoria, Australia

^b The Melbourne Centre for Nanofabrication, Clayton, 3168 Victoria, Australia

**Corresponding author: Wenlong.Cheng@monash.edu*

Supporting Notes

1. Calculation of the specific capacitance of v-AuNWs sponge based supercapacitors

The volumetric specific capacitances (C_v) were calculated based on a cyclic voltammetry curve as following:

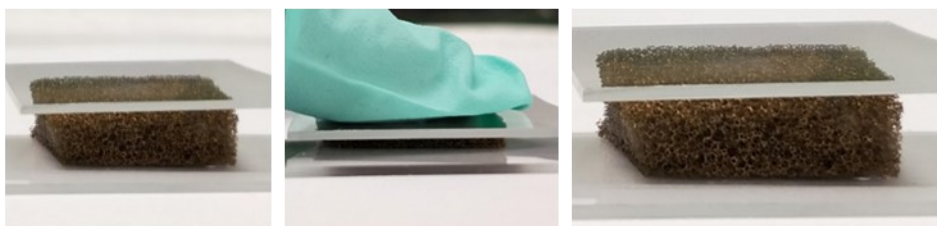
$$C_v = \frac{\int i dV}{2\nu\Delta Vv} \quad (1)$$

where ν is the scan rate (unit is mV s^{-1}), ΔV is the potential window (0.8 V), v is the volume of v-AuNWs sponge based supercapacitor (unit is cm^3).

Materials	compressibility	bending	Stretchability	stability	ref
PANI/SWCNT sponge	60%	N/A	N/A	92% (1000 cycles)	1
Co(OH)F/ PEDOT:PSS/AgNW sponge	N/A	120°	N/A	86% (3000 cycles)	2
CNT/PDMS sponge	50%	N/A	N/A	98% (3000 cycles)	3
NiCo ₂ S ₄ carbon sponge	60%	N/A	N/A	90% (3000 cycles)	4
nitrogen (N)-doped carbon foams	60%	N/A	N/A	96% (4000 cycles)	5
CNT sponge/PPy/MnO ₂	50%	N/A	N/A	90% (1000 cycles)	6
v-AuNWs/PANI sponge	50%	180°	66%	93% (1000 cycles)	Our work

Table S1. Summary of sponge-based flexible supercapacitors reported in literature.

A



B

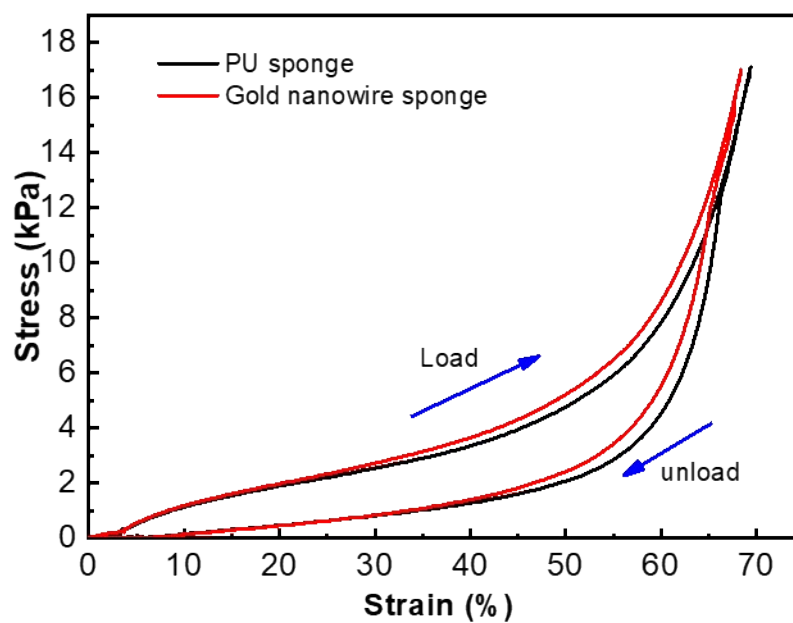


Figure S1. (A) Photographs of compressible v-AuNWs sponge. (B) Compressible stress–strain curves for sponge and v-AuNWs sponge.

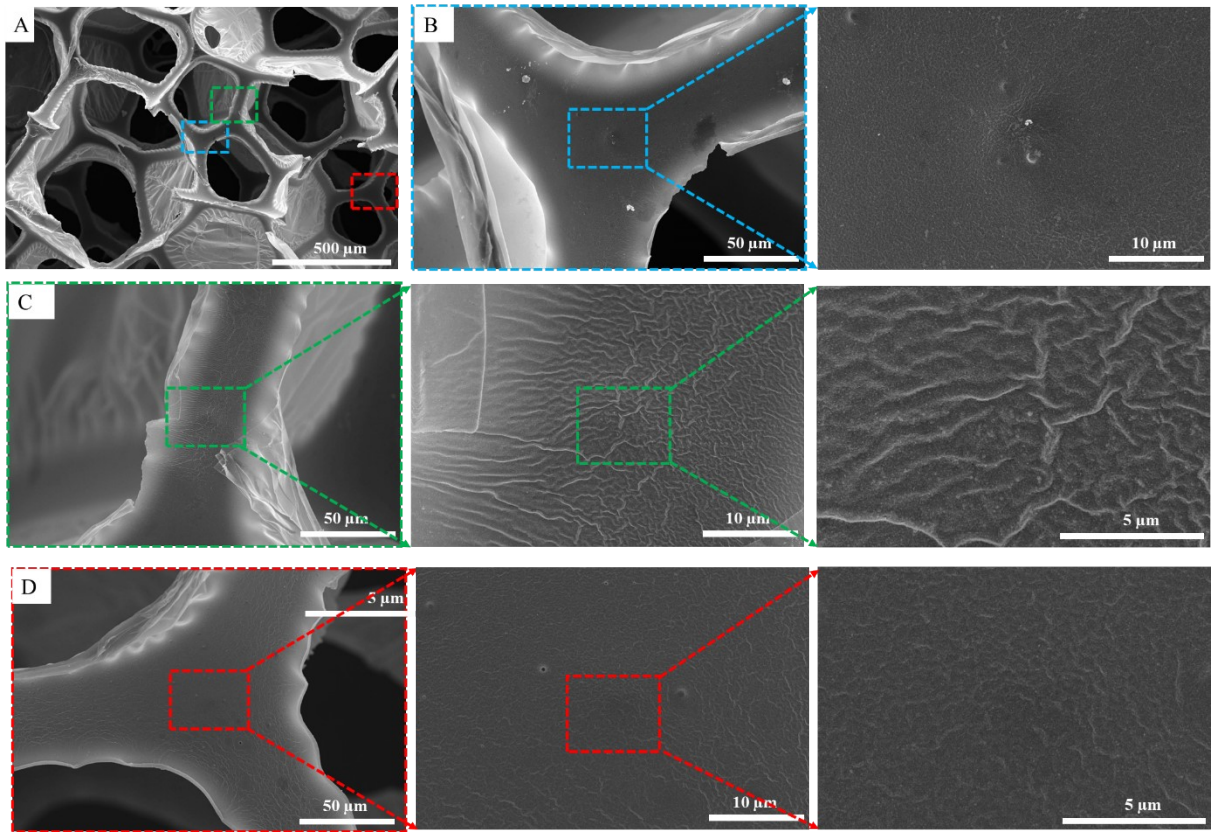


Figure S2. (A) SEM image of v-AuNWs sponge without any Ecoflex embedment and external deformations; we chose three areas, marked in color dashed rectangles, zoom in and find out details in (B), (C) and (D).

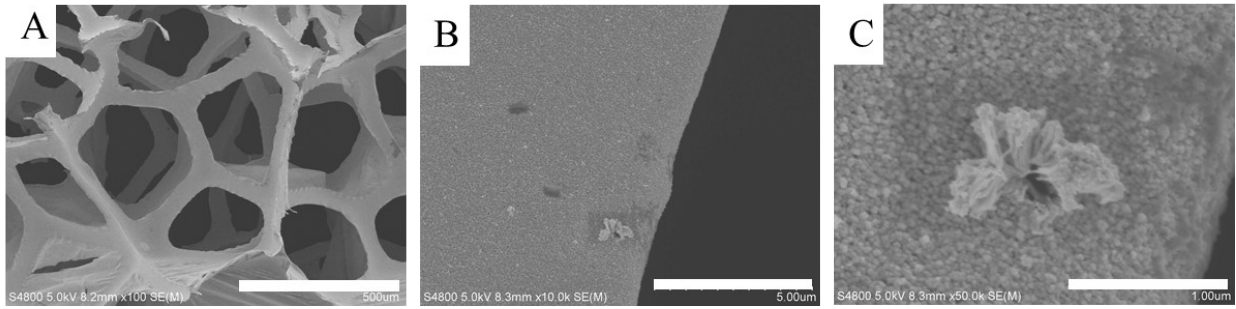


Figure S3. SEM image of v-AuNWs sponge without any Ecoflex embedment and external deformations under different magnifications, the scale bar is 500 μm (A), 5 μm (B) and 500 nm (C) respectively.

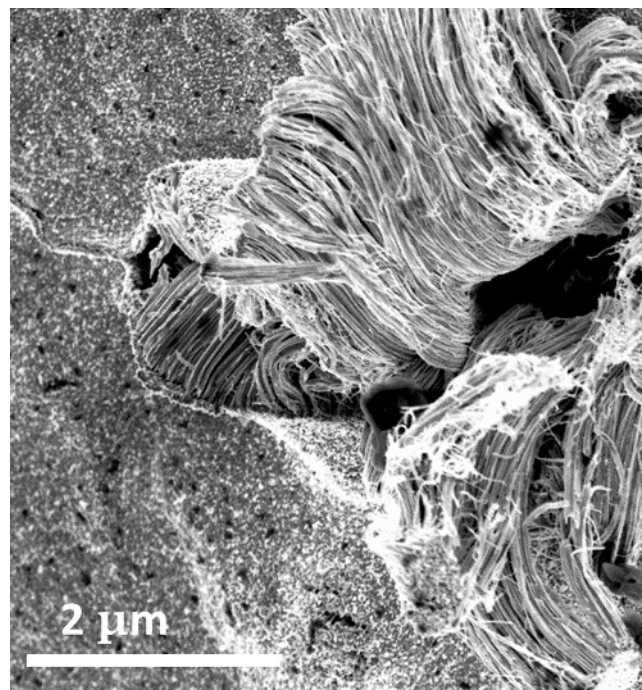


Figure S4. SEM image of v-AuNWs on sponge skeleton with a nanowire length of $\sim 2 \mu\text{m}$. Scale bar is $2 \mu\text{m}$. This particular v-AuNWs sponge was fabricated by immersing Au seed modified sponge into the growth solution of ethanol/water ($v/v = 1:1.2$), including HAuCl₄ (12 mM), ligand MBA (1.1 mM), and L-AA (30 mM) for 15 minutes.

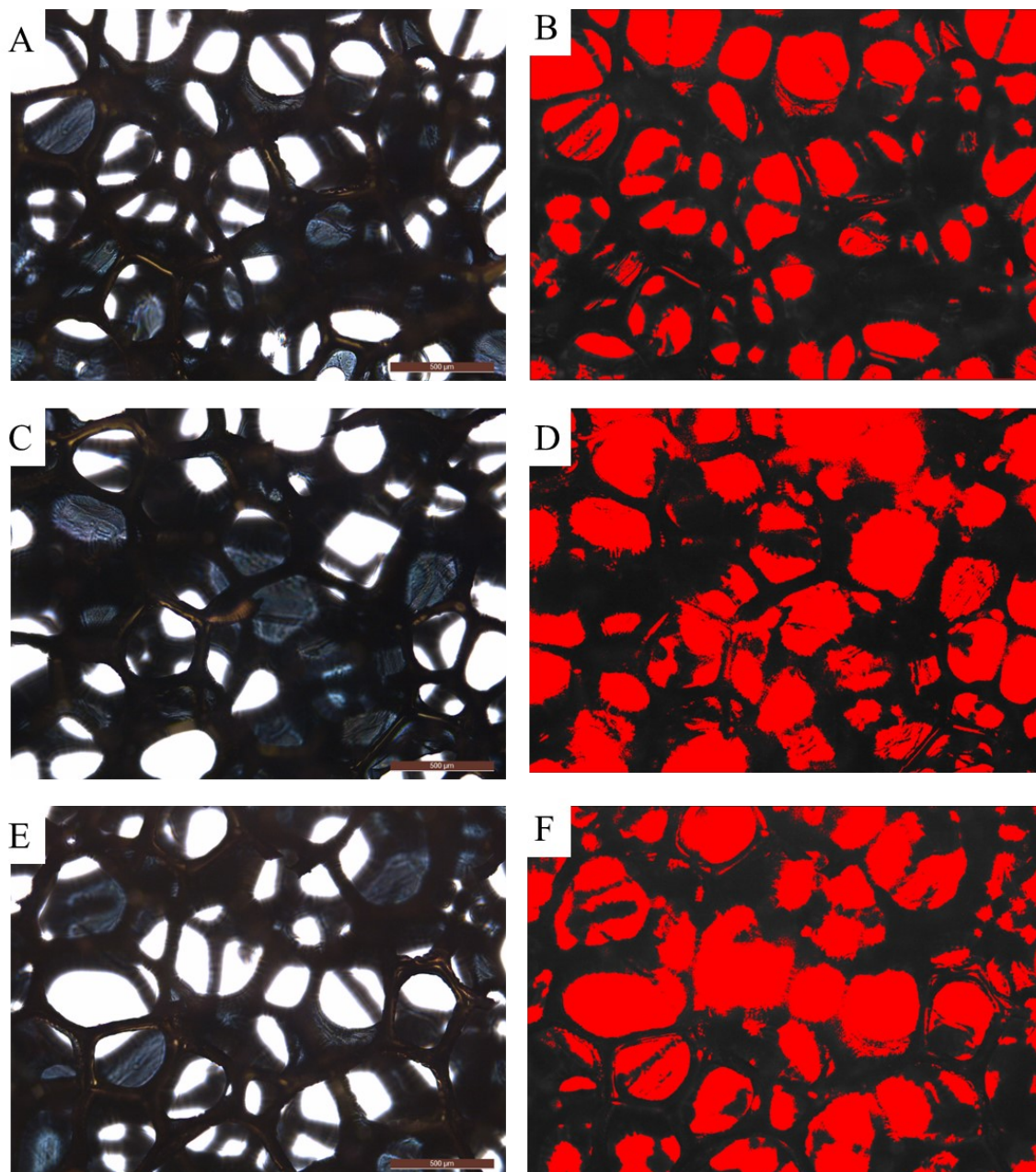


Figure S5. (A, C, E) Optical images of v-AuNWs sponge without Ecoflex embedment (the size is 1 cm × 1 cm × 0.5 cm). (B, D, F) Particles analysis of (A), (C), (E), respectively. The unoccupied spaces are dyed with red color by the software image J.

The three random cross-sectional images were taken in order to estimate the porosity. The raw optical images were undertaken particle analysis with the software (Image J). The parts in black are the v-AuNWs sponge skeletons; the unoccupied parts in red are the porous cross-sectional area. The estimated porosity of v-AuNWs sponge was $50.3 \pm 2.4\%$.

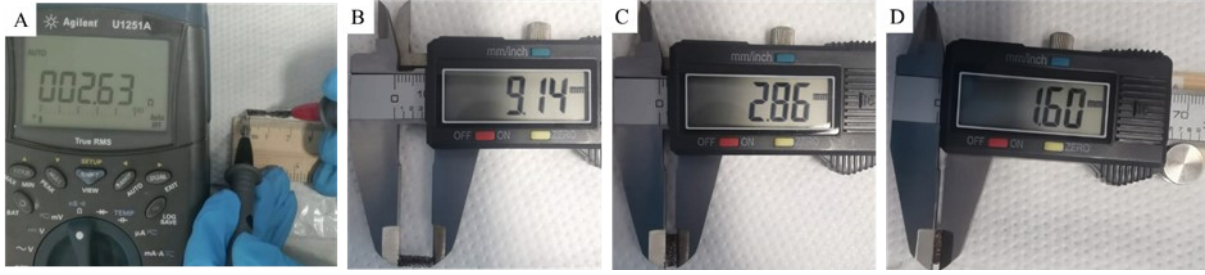


Figure S6. (A) The resistance of v-AuNWs sponge. (B) The length of this v-AuNWs sponge. (C) The width of this v-AuNWs sponge. (D) The thickness of this v-AuNWs sponge.

Calculation the conductivity of v-AuNWs sponge

The conductivity of v-AuNWs sponge was calculated as follow:

$$\rho = R \frac{A}{L} \quad (3)$$

$$\sigma = \frac{1}{\rho} = \frac{L}{RA} \quad (4)$$

where σ is conductivity (unit is $S m^{-1}$), ρ is the resistivity (unit is $\Omega.m$), R is the electrical resistance (unit is Ω), L is the length (unit is m), A is the cross-section area (unit is m^2) of the sample. This gives the estimation of apparent conductivity. If the porous area in the cross-section area was excluded, the effective area occupied by skeleton should be considered. Then the effective conductivity should be

$$\sigma = \frac{L}{RA(1 - \varepsilon)} \quad (5)$$

where ε is cross-sectional porosity.

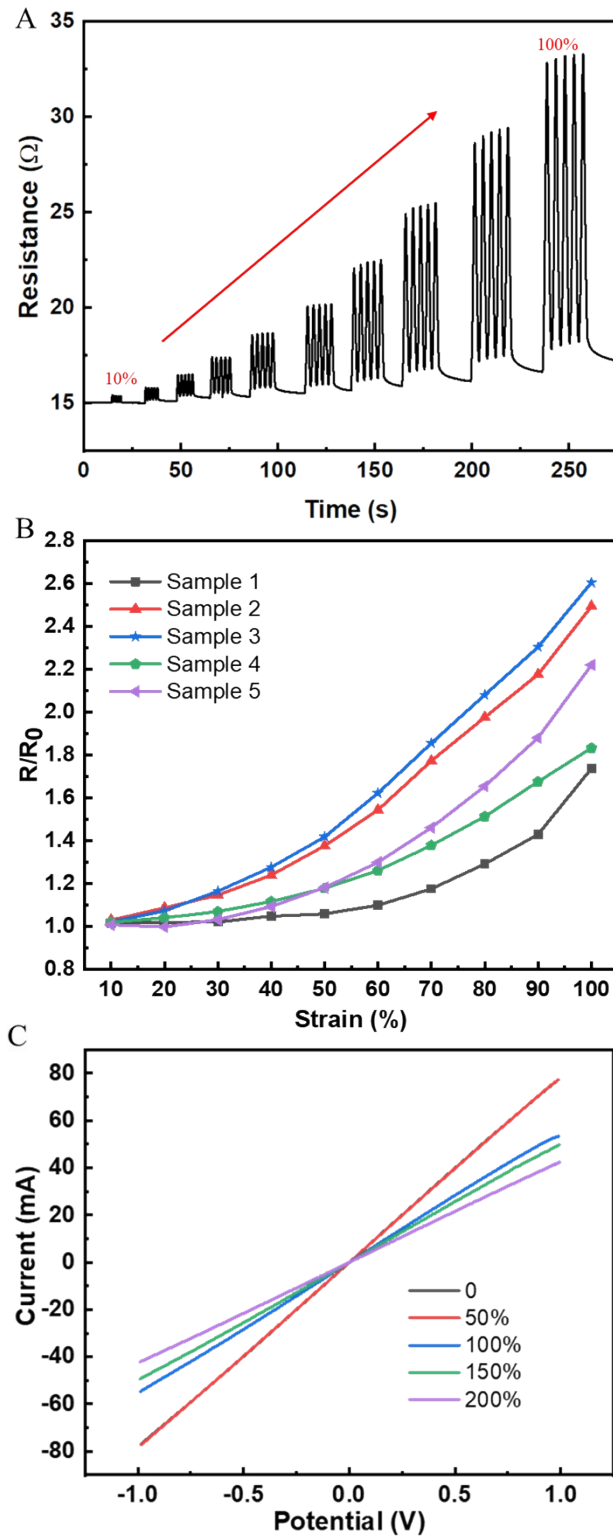


Figure S7. (A) Resistance of v-AuNWs sponge/ Ecoflex composite under different strains from 10% strain to 100% strain, each applied strain test 5 cycles. (B) Summary of five v-AuNWs sponge/Ecoflex

composites samples resistance change under different strains from 10% to 100% strain. (C) I-V curves test from one v-AuNWs sponge/Ecoflex composite sample at different strain levels.

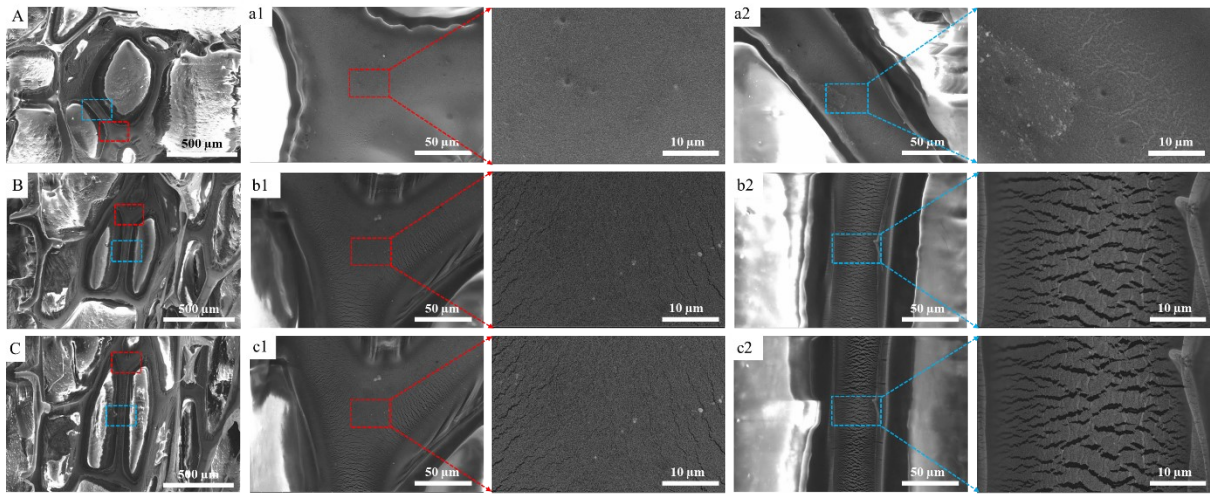


Figure S8. SEM images of v-AuNWs sponge/ Ecoflex conductor under no strain (A), 30% strain (B), and 100% strain (C); (a1) and (a2) are the zoom in view of red and blue dashed rectangles in (A) respectively; (b1) and (b2) are the zoom in view of red and blue dashed rectangles in (B) respectively; (c1) and (c2) are the zoom in view of red and blue dashed rectangles in (C) respectively. (B) and (C) are from same sample and almost same areas.

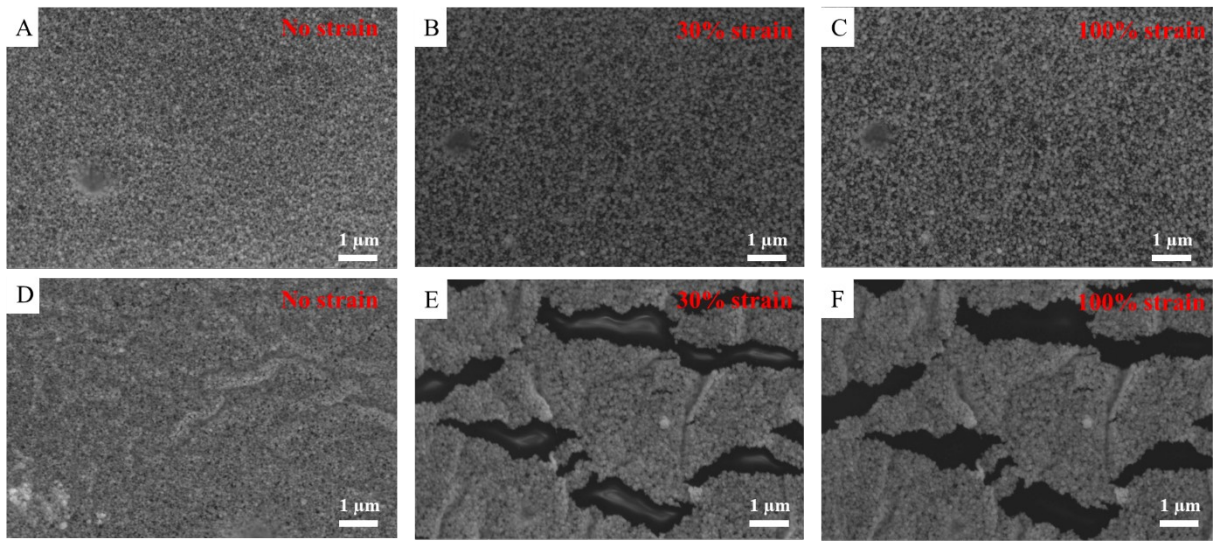


Figure S9. (A-F) SEM images of zoom in view of (a1), (b1), (c1), (a2), (b2), (c2) in figure S7 respectively.

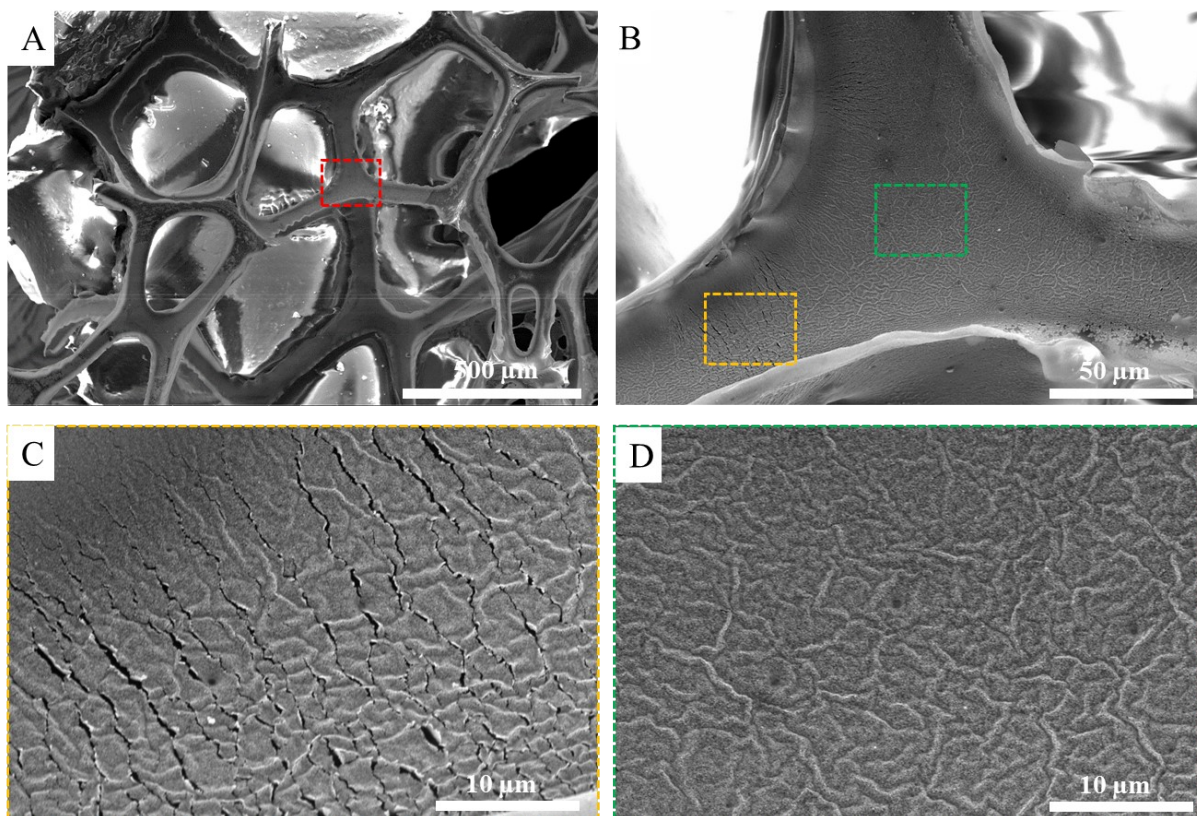


Figure S10. SEM images of v-AuNWs sponge/ Ecoflex conductor after 5000 stretching cycles (A); (B) is the zoom in view of red dashed rectangle in (A); (C) and (D) are the zoom in view of yellow and blue dashed rectangles in (B).

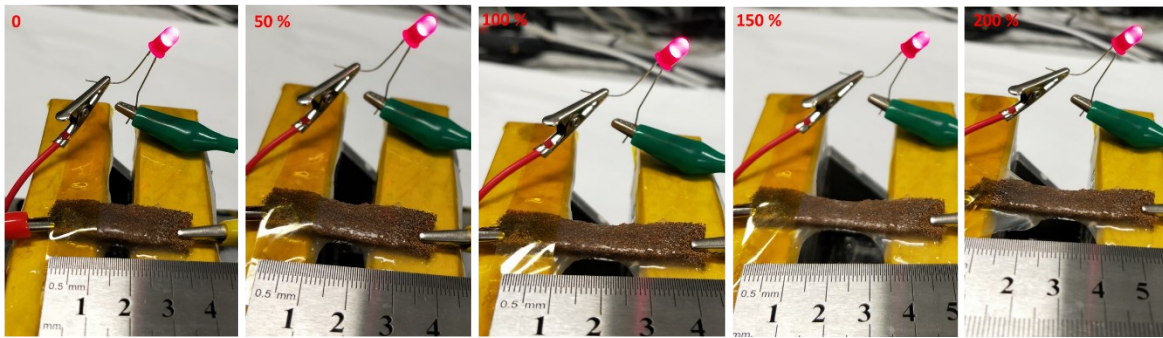


Figure S11. Photograph of v-AuNWs sponge/Ecoflex conductor under different strain levels.

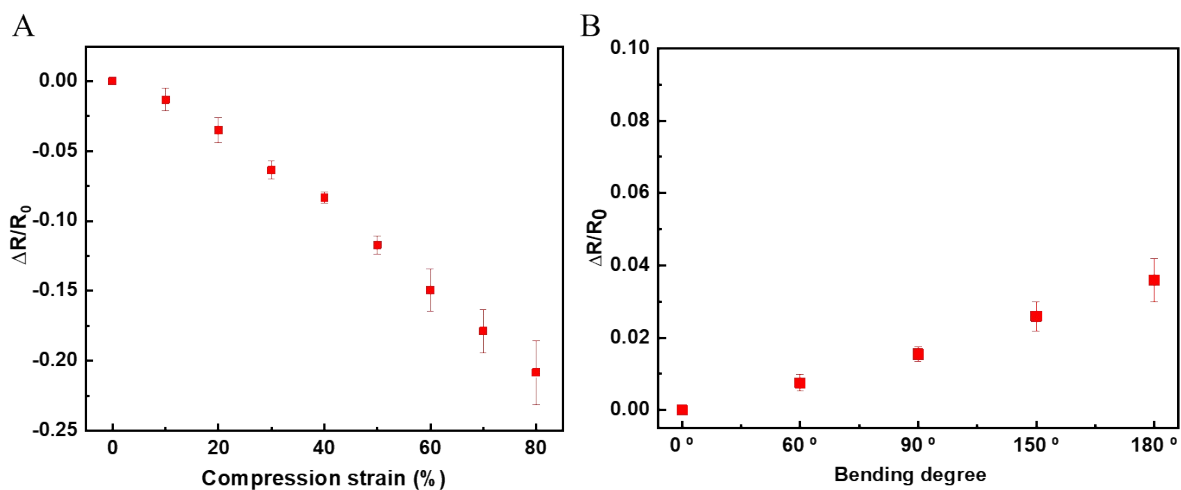


Figure S12. (A) The relative resistance change of v-AuNWs sponge under different compression strains. (B) The relative resistance change of v-AuNWs sponge under different bending degrees. Both results obtained from three samples and each sample tested two times. The $\Delta R/R_0=(R-R_0)/R_0$, in which the R_0 is the resistance when no external deformation applied to the v-AuNWs sponge, and R is the resistance when different external deformations applied to the v-AuNWs sponge.

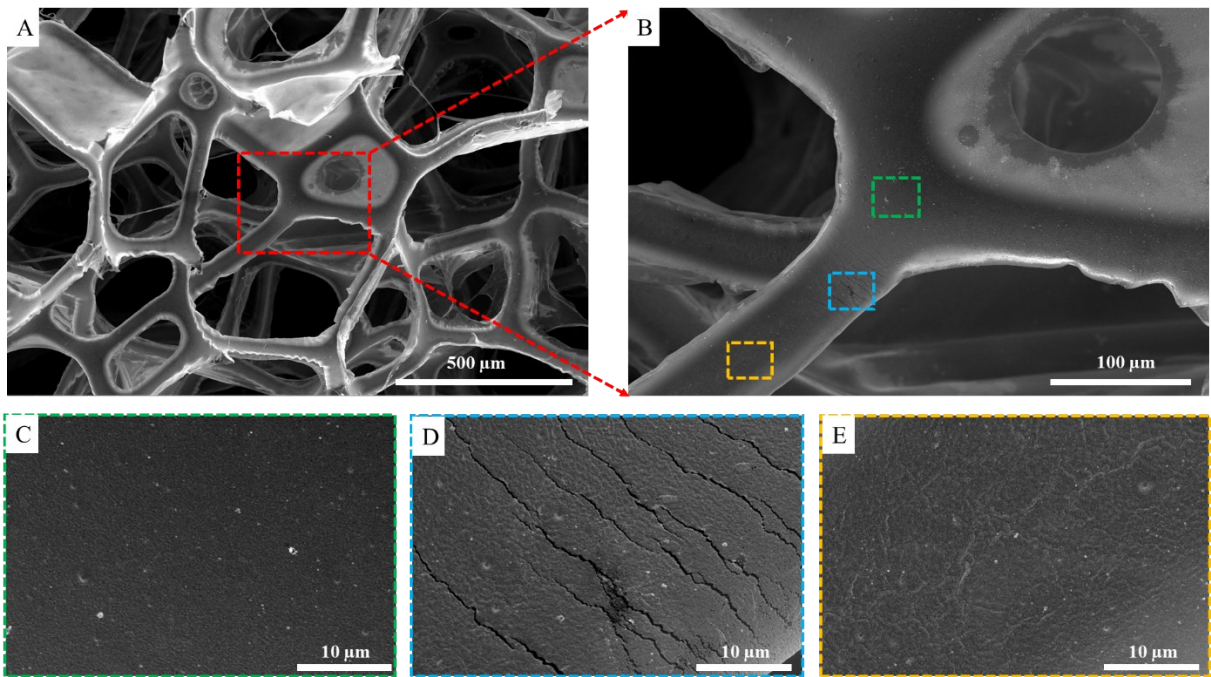


Figure S13. (A) SEM images of v-AuNWs sponge without Ecoflex under 50% compression; (B) is the zoom in view of red dashed rectangle in (A); (C), (D) and (E) are the zoom in view of green, blue and yellow dashed rectangles in (B) respectively.

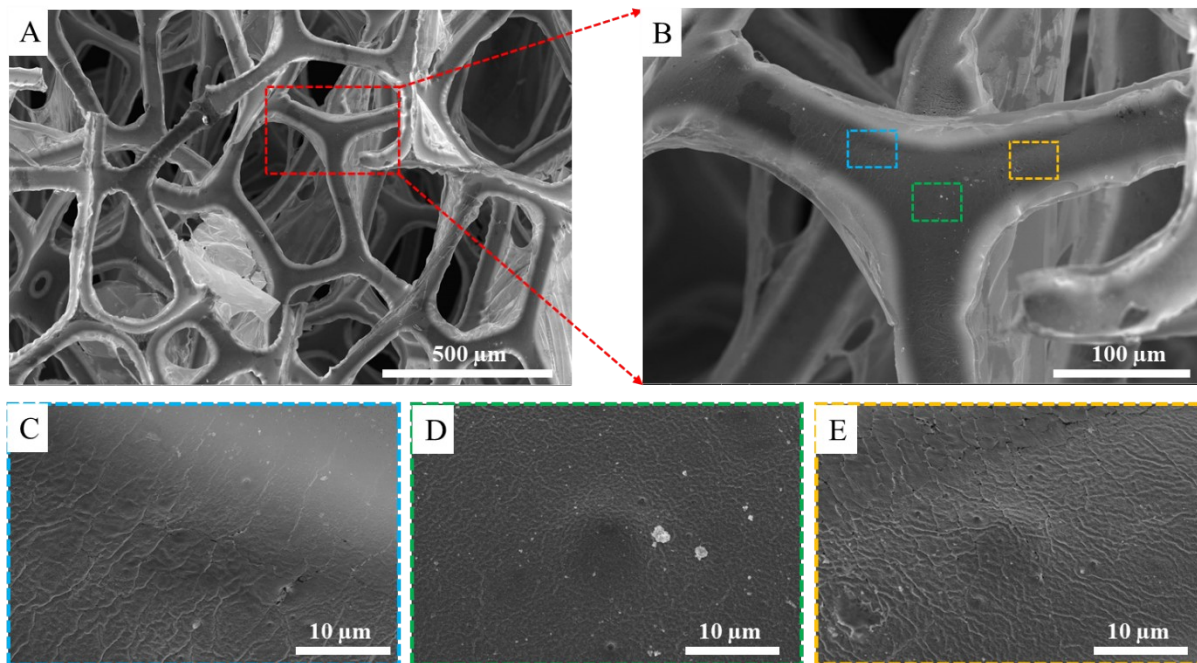


Figure S14. (A) SEM images of v-AuNWs sponge without Ecoflex after 50% compression cycles for 20 times; (B) is the zoom in view of red dashed rectangle in (A); (C), (D) and (E) are the zoom in view of blue, green and yellow dashed rectangles in (B) respectively.

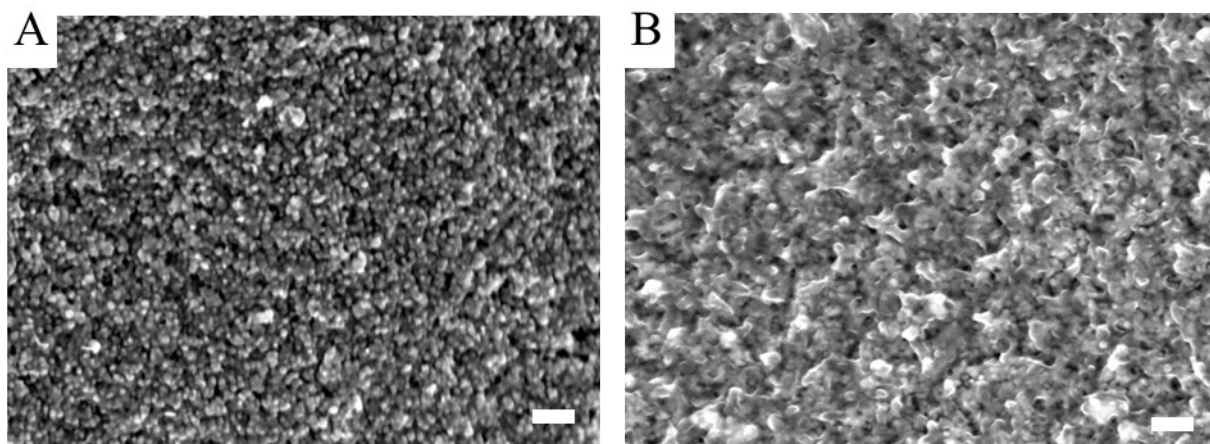


Figure S15. SEM images of v-AuNWs sponge before (A) and after (B) PANI deposition, scale bar is 100 nm. Sample for A is v-AuNWs sponge, sample for B is PANI deposited on v-AuNWs sponge.

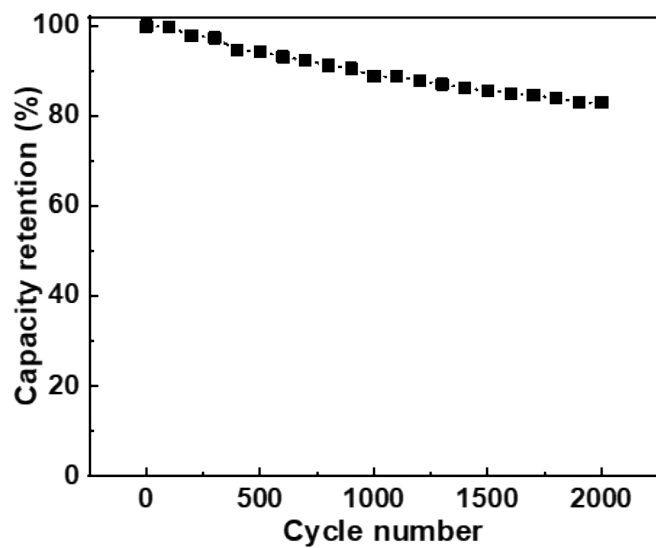


Figure S16. Capacitance retention of v-AuNWs/PANI sponge based supercapacitor for 2000 CV cycles under 200 mV s^{-1} scan rate.

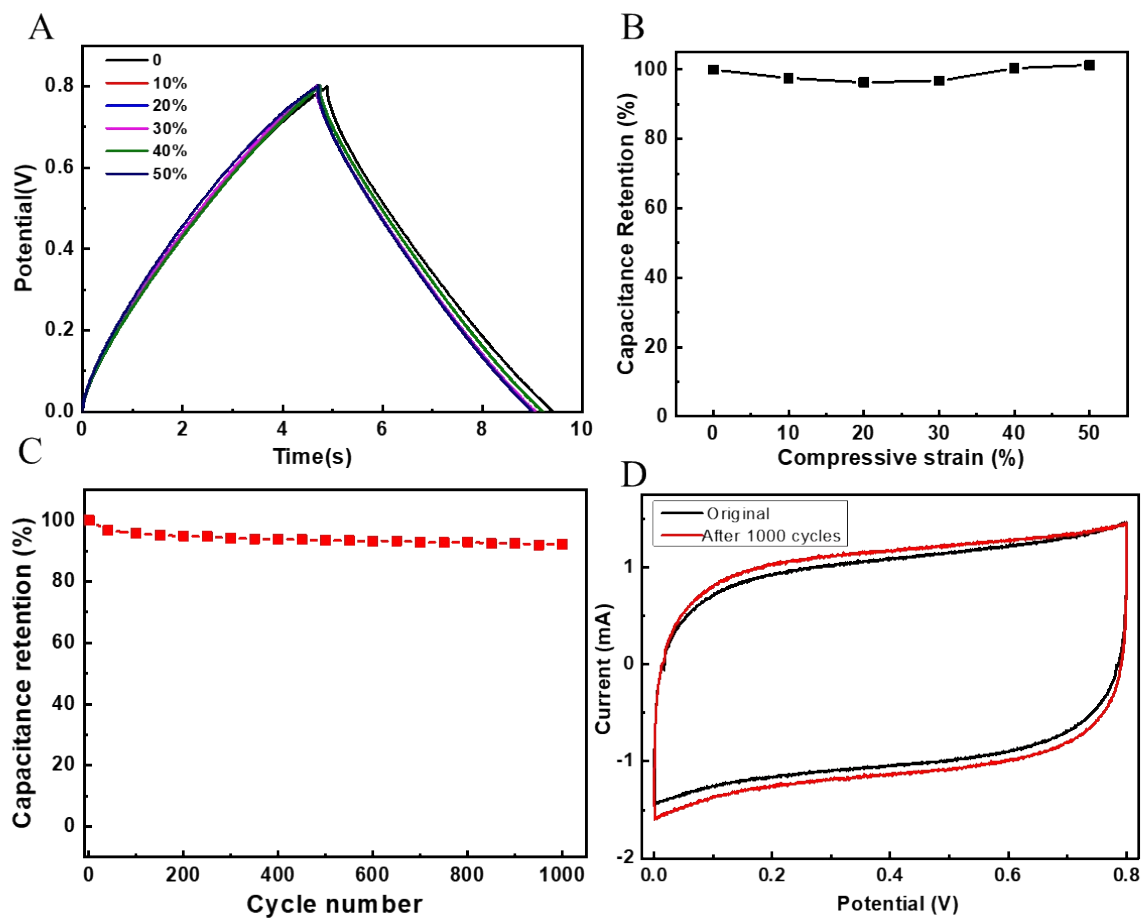


Figure S17. (A) GCD curves of v-AuNWs/PANI sponge based supercapacitor under different compression strains. (B) Capacitance retention under different compression strains. (C) Capacitance retention under repeated compressing 50% for 1000 cycles. (D) CV curves under 200 mV s^{-1} before and after 1000 compressing tests.

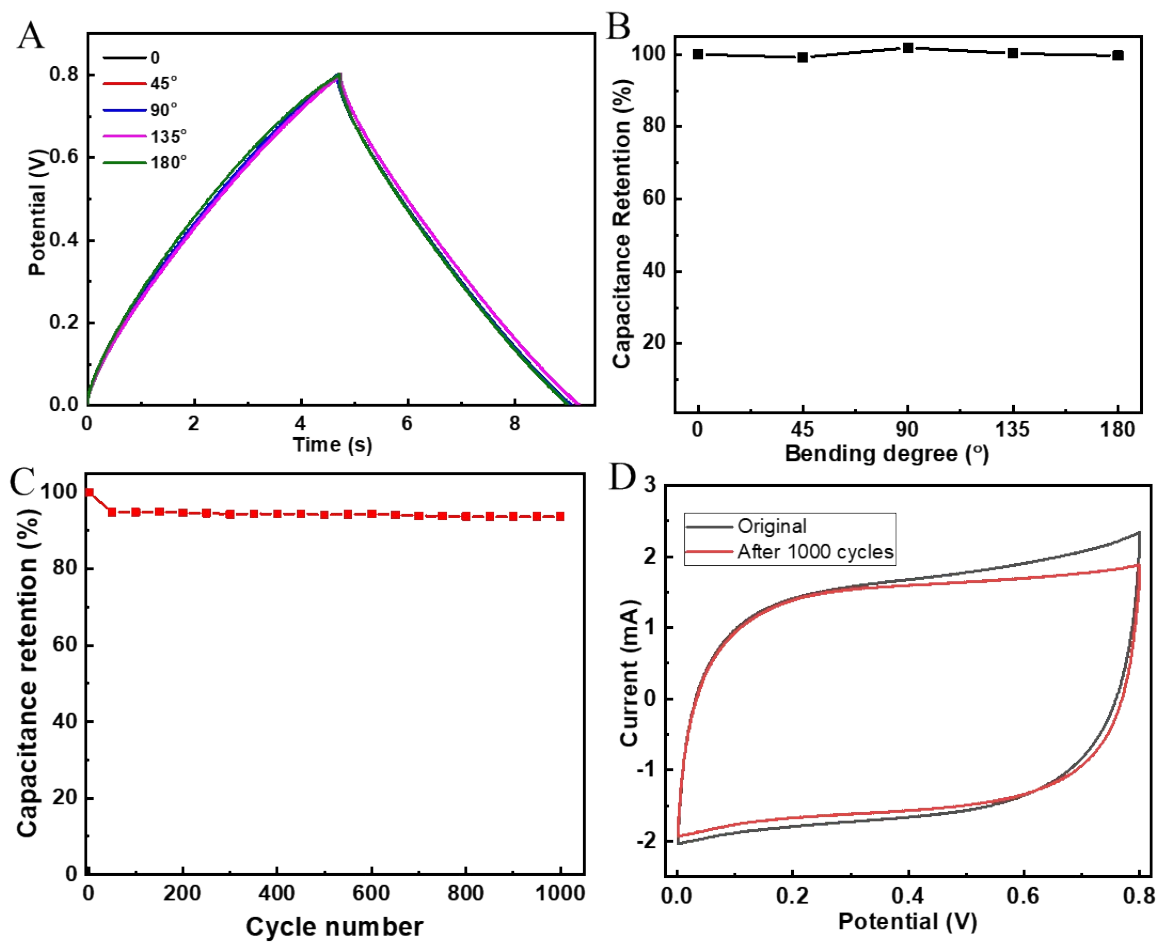


Figure S18. (A) GCD curves of v-AuNWs/PANI sponge based supercapacitor under different bending degrees. (B) Capacitance retention under different bending degrees. (C) Capacitance retention under repeated bending to 180° for 1000 cycles. (D) CV curves under 200 mV s⁻¹ before and after 1000 bending tests.

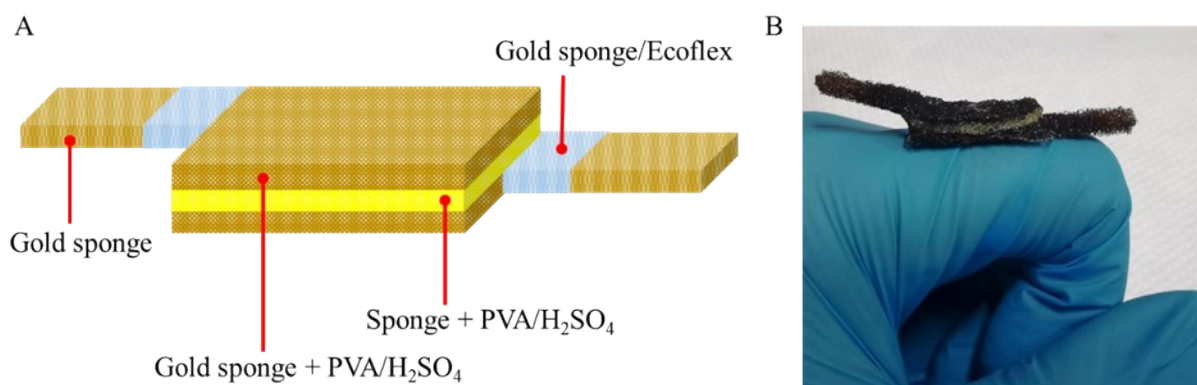


Figure S19. (A) Scheme of gold nanowires sponge based fully deformable supercapacitors. (B) Photograph of fully deformable gold nanowires sponge based supercapacitors.

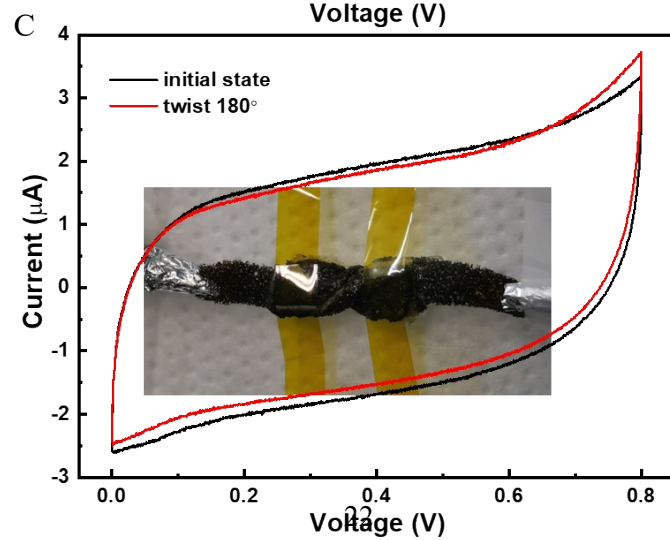
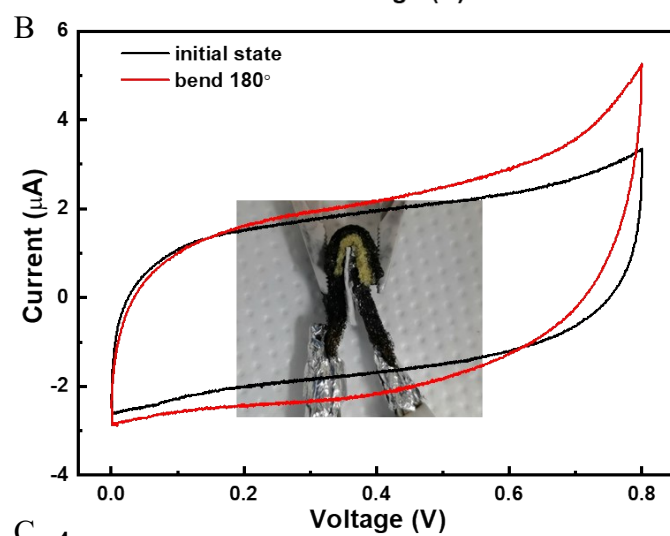
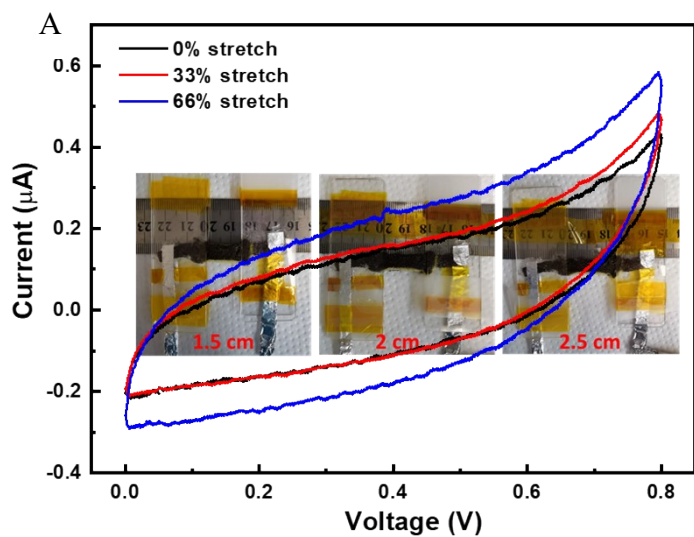


Figure S20. Electrochemical performance of fully soft v-AuNWs sponge-based supercapacitors under stretching (A), bending (B), and twisting (C), the insert optical images are v-AuNWs sponge based supercapacitors under stretching, bending, and twisting respectively.

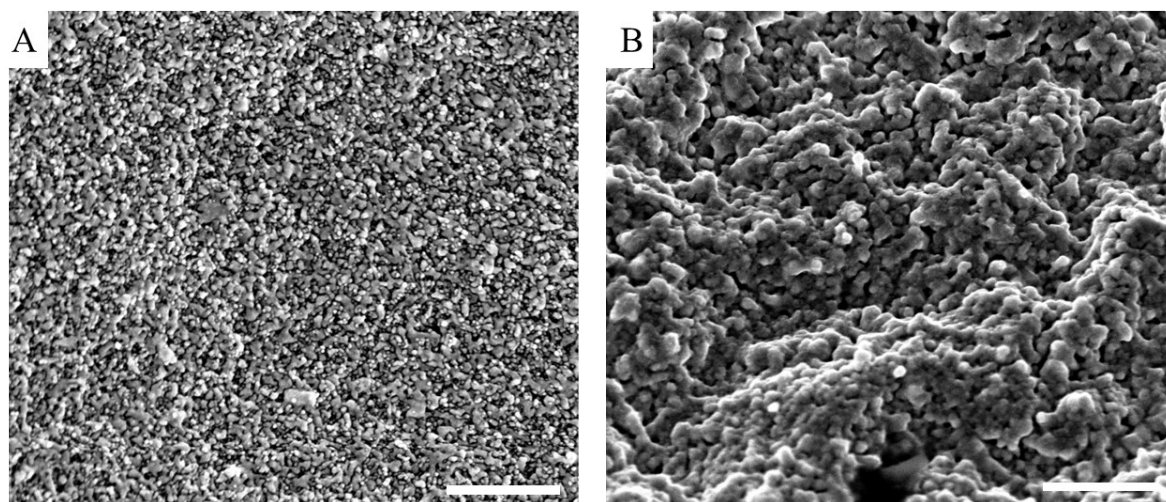


Figure S21. SEM image of v-AuNWs sponge before (A) and after (B) catalysis, scale bas is 500 nm. Sample for A is v-AuNWs sponge, sample for B is v-AuNWs sponge after catalysis.

References

1. Z. Niu, W. Zhou, X. Chen, J. Chen and S. Xie, *Adv. Mater.*, 2015, **27**, 6002-6008.
2. I. K. Moon, S. Yoon and J. Oh, *Adv. Mater. Interfaces*, 2017, **4**, 1700860.
3. Y. Song, H. Chen, Z. Su, X. Chen, L. Miao, J. Zhang, X. Cheng and H. Zhang, *Small*, 2017, **13**, 1702091.
4. X. Liang, K. Nie, X. Ding, L. Dang, J. Sun, F. Shi, H. Xu, R. Jiang, X. He, Z. Liu and Z. Lei, *ACS Appl. Mater. Interfaces*, 2018, **10**, 10087-10095.
5. K. Xiao, L. X. Ding, G. Liu, H. Chen, S. Wang and H. Wang, *Adv. Mater.*, 2016, **28**, 5997-6002.
6. P. Li, Y. Yang, E. Shi, Q. Shen, Y. Shang, S. Wu, J. Wei, K. Wang, H. Zhu, Q. Yuan, A. Cao and D. Wu, *ACS Appl. Mater. Interfaces*, 2014, **6**, 5228-5234.